Arch. Metall. Mater., Vol. 61 (2016), No 1, p. 209–212

DOI: 10.1515/amm-2016-0038

A. DOBKOWSKA*#, B. ADAMCZYK – CIEŚLAK*, J. MIZERA*, K. J. KURZYDŁOWSKI*, A. KIEŁBUS**

# THE COMPARISON OF THE MICROSTRUCTURE AND CORROSION RESISTANCE OF SAND CAST ALUMINUM ALLOYS

The influence of different types of precipitation on the corrosion behavior was investigated in three aluminum–silicon-magnesium alloys. The microstructures of the alloys were studied through optical (OM) and scanning electron microscopy (SEM). The structures consisted of an α-Al solid solution matrix, Si eutectic crystals, secondary phases AlFeSi and AlMgFeSi (Chinese script), as well as $Mg_2Si$. The corrosion behavior was examined with the use of a potentiodynamic polarization test followed by a SEM surface analysis. The results indicate that all the analyzed samples were in the passive state and AlSi10Mg was less reactive in the corrosive environment.

*Keywords*: aluminium-silicon-magnesium alloys, microstructure, corrosion

## 1. Introduction

Aluminum alloys, because of their low mass and good mechanical properties, are one of the most popular groups of functional materials. AlSi5, AlSi7Mg and AlSi10Mg are typical casting alloys used for parts with thin walls and complex geometry. This kind of alloy is also used for parts which are subject to high loads and are complicated in shapes. Due to the complicated shape and size, the elements are produced mostly by sand casting. The properties of the aluminum–silicon alloys depend on the amount of the alloying elements in the microstructure. The microstructure of these alloys is built from an α–aluminum solid solution and secondary phases such as AlFeSi, AlFeSiMn, $Mg_2Si$, AlFeSiMg. As it is known one of the most problematic properties of these kinds of alloys is the corrosion resistance. The most common form of aluminum corrosion is pitting, especially when chloride ions are present, causing the breakdown of the passive layers. Due to the corrosion processes in the aluminum–silicon alloys, the silicon is cathodic in relation to the aluminum matrix. That is why localized micro galvanic corrosion can be observed. Defects formed during the casting processes also have an influence on the course of the corrosion mechanisms. The corrosion mechanism is more complicated when other types of phases are present in the microstructure [1 - 6]. The aim of this work is to compare the corrosion resistance of the AlSi5, AlSi7Mg and AlSi10Mg alloys.

## 2. Methods

Metallographic observations were performed with the use of optical microscopy (OM). The metallographic samples were prepared by means of the standard metallographic procedure, which includes cutting, mounting, grinding and polishing. The samples were ground (600 – 1200 grit papers), mechanically polished and etched with the use of the Keith etching reagent. The corrosion resistance of these alloys was characterized by means of the Potentiodynamic Polarization Test (PPT), with the use of the AutoLab equipment with a three electrode system. A saturated calomel electrode (SCE) was the reference electrode and a platinum electrode was the counter electrode. The tests were conducted in 0.1 M sodium chloride (0.1 M NaCl) at room temperature. The scan rate was 0.1 mV/s and the potential range was from -1 to 2 V. The examination of the corrosion attack morphology as well as the EDS analysis were performed with the use of scanning electron microscopy with an energy dispersive spectrometer (SEM/EDS) in the secondary electron and the backscattered electron mode. SEM investigations were performed with the use of 3500 N with an accelerating voltage of 15 kV.

## 3. Results

The results of the metallographic observations performed by means of an optical microscope show that all of the investigated cast aluminum alloys are characterized by a dendritic structure of the solid solution (α) (Figs 1a, 2a, 3a) and a discontinuous Si (β) phase forming α+β eutectic grains (Fig. 1b).

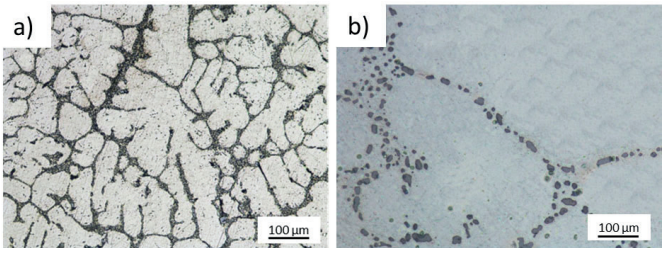


Fig. 1. Structure of the AlSi5 alloy as observed (light microscope)

* WARSAW UNIVERSITY OF TECHNOLOGY, FACULTY OF MATERIALS SCIENCE AND ENGINEERING, 141 WOLOSKA STR., WARSZAWA, POLAND

** SILESIAN UNIVERSITY OF TECHNOLOGY, DEPARTMENT OF PHYSICS AND CHEMISTRY OF METALS, 12 BANKOWA STR., KATOWICE, POLAND

# Corresponding author: anna.dobkowska@inmat.pw.edu.pl

As we can see, the morphology depends on the concentration of the silicon mass. Also, a plate/needle-like morphology of the particle is visible (Fig. 2a). The analysis of the literature data revealed that the needle-like particles are probably intermetallic, e.g. β-$Al_5FeSi$ [7 – 16]. Also, the occurrence of the script-type phases (Fig. 3b), such as α-AlFeMnSi and π-AlFeMgSi is visible, especially in the AlSi7Mg and AlSi10Mg alloys. What is more, in these alloys "bone" particles of the magnesium phase $Mg_2Si$ were detected (Fig. 2b). As the literature data shows, the presence of the β-AlFeSi intermettalic phase has an adverse influence on the properties of the aluminum–silicon-magnesium alloys [17]. This phase is visible as needles in the structure, and the shape of this phase depends on the amount of iron in the microstructure. β-AlFeSi has got a low adhesion to the matrix. To reduce the presence of this phase in the microstructure, Mn is added as an alloying element. The addition of Mn has an influence on the formation of the AlFeSiMn phase. The AlFeSiMn phase significantly improves the mechanical or corrosive properties of the material [18].

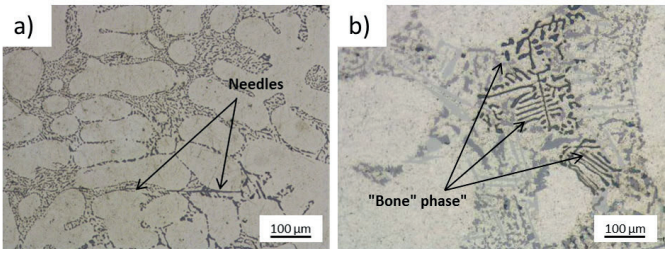


Fig. 2. Structure of the AlSi7Mg alloy as observed (light microscope)

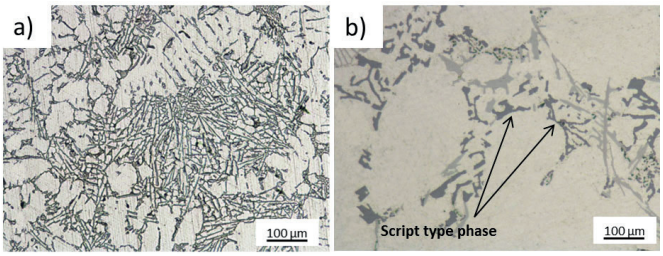


Fig. 3. Structure of the AlSi10Mg alloy as observed (light microscope)

In order to confirm the assumptions about the composition of the intermetallic phases, the spectral analysis of selected phases was performed. The EDS analysis results (Fig. 4a) showed that the positions 1, 3 and 6 were defined as the eutectic silicon phase. The analysis of the positions 4 and 5 shows a phase containing magnesium, iron, silicon and aluminum, which, taking into account its morphology, may be considered as the $Al_9FeMg_3Si_5$ phase. The position 2, beside the aluminum content, also showed silicon and iron, yet a very low manganese content. The EDS studies confirmed the presence of the β-AlFeSi platelets (without Mn) and the α-AlFeMnSi phase with the addition of manganese. Fig. 4b analyzes a phase containing magnesium and silicon, as positions 1 and 2. It may be considered as the Mg2Si phase and it confirms the original assumption. Fig. 5a shows the analysis for AlSi10Mg where the phase containing Mn is observable. Positions marked as 1 and 2 (Fig. 5a) show phase containing magnesium, aluminum, manganese and iron. It could confirm the presence of α-AlFeMnSi phase which properties were mentioned above. The results shown in the Fig. 5b marked as 1 and 2 contain small share of aluminum and in the majority of silicon which confined the presence of eutectic silicon phase. Besides Mg2Si and π-AlFeMgSi were also identified in the microstructure of AlSi10Mg alloy.

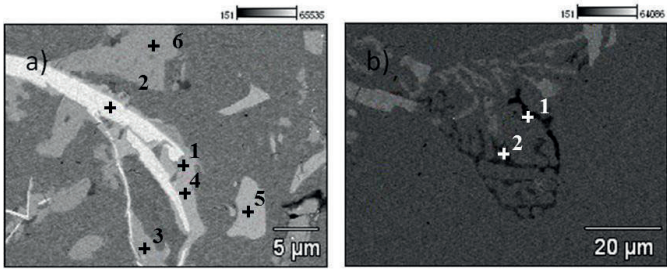


Fig. 4. SEM micrographs of the AlSi7Mg alloy and the positions of the EDS analysis

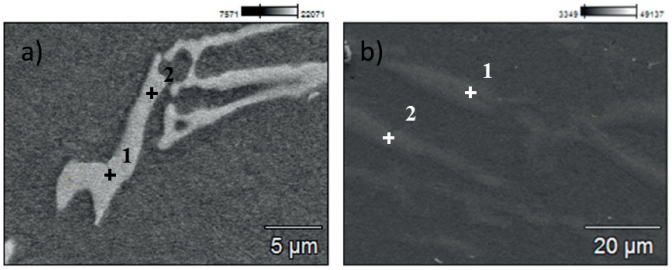


Fig. 5. SEM micrographs of the AlSi10Mg alloy and the positions of the EDS analysis

The polarization curves of AlSi5, AlSi7Mg and AlSi10Mg after the potentiodynamic tests in a 0.01 M NaCl solution are shown in Fig. 6. The polarization curves of all the experimental alloys are similar. The cathode and anode branches of the polarization curves are not symmetrical. The potentiodynamic anodic curves show that the analyzed materials are in the passive state and undergo pitting corrosion.

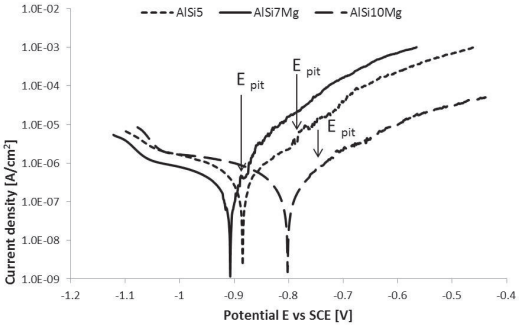


Fig. 6. Potentiodynamic polarization curves obtained for the AlSi5, AlSi7Mg and AlSi10Mg alloys.

Fig. 6. Potentiodynamic polarization curves obtained for the AlSi5, AlSi7Mg and AlSi10Mg alloys

The values of the corrosion potential Ecor are from -0.91 V for AlSi7Mg and -0.89 for AlSi5 up to -0.82 V for AlSi10Mg (Tab. 1). This shift in the corrosion potential is connected with several factors, such as the type of precipitates present in the microstructure. As it well known the presence of different microstructural features in the alloys can cause microgalvanic corrosion. As the silicon particles are cathodic in relation to the eutectic aluminum phase, the corrosion processes should mostly

occur in the areas where the silicon particles are surrounded by this phase [1 – 4]. There are differences in the current density icor, where the values are from 6.38e-8 A/cm$^2$ for AlSi7Mg up to 1.606e-7 A/cm$^2$ for AlSi5 and 1.034e-7 A/cm$^2$ for AlSi10Mg. The growth of the current density in the anodic range and the small differences between the pitting potential $E_{pit}$ and the corrosion potential $E_{cor}$ indicate insignificant stabilization of the passive layer. The effect is well observable on the AlSi10Mg sample, where the obtained values of the potential ($E_{cor}$ and $E_{pit}$) are similar. The distribution of the intermetallic phases, the distribution of Si in the structure, the thickness of the corrosion layers and the pores present in the microstructure can have a strong influence on this effect.

TABLE 1
Characteristic electrochemical parameters of the analyzed alloys obtained by the potentiodynamic method

| Sample | $i_{cor}$[A/cm$^2$] | $E_{cor}$[V] | $E_{pit}$ |
|---|---|---|---|
| AlSi5 | 1.606e-7 | -0.89 | -0.79 |
| AlSi7Mg | 6.38e-8 | -0.91 | -0.89 |
| AlSi10Mg | 1.034e-7 | -0.82 | -0.75 |

SEM observations present in Fig. 7 show difference between progressive corrosion damages of AlSi5, AlSi7Mg and AlSi10Mg. As it is observable the smallest damages after corrosion tests occurred on the surface of AlSi10Mg. From the corrosive point of view, Mn reduces the cathodic effect of the iron. This has an impact on the galvanic processes and leads to less intense galvanic couples compared with the Al-Fe-Si intermetallic compounds. That is why AlSi10Mg has got smaller reactivity in the corrosive solution.

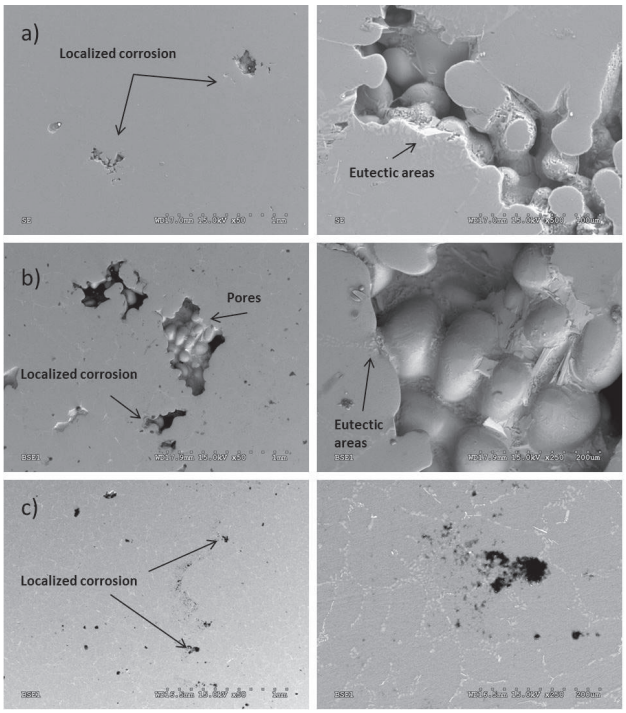


Fig. 7. SEM images of the morphology after potentiodynamic polarization measurements obtained for: a) AlSi5, b) AlSi7Mg, c) AlSi10Mg.

## 4. Conclusions

In this work the microstructure and its influence on corrosion resistance of AlSi5, AlSi7Mg and AlSi10Mg was described. The microstructure observations and the example of EDS studies of the AlSi7Mg and AlSi10Mg alloys confirmed the presence of the α-Al matrix, the Si particles, the α-AlFeMnSi and β-AlFeSi intermetallic phases, as well as the π-AlFeSiMg phase and a small amount of Mg2Si particles. The AlFeMnSi phase was also observable in the microstructure of AlSi10Mg. In the case of the AlSi5 alloy, the presence of the $Mg_2Si$ particles was not visible.

Laboratory tests of corrosion behavior of analyzed materials in 0.1 M NaCl showed that all materials underwent localized corrosion. Pits are well observable on the surface of samples and there are differences in their depth and volume. Because of different microstructural features observed in materials there are differences in corrosion resistance of AlSi5, AlSi7Mg and AlSi10Mg. The less reactive in 0.1 M NaCl was AlSi10Mg where the phases containing Mn are present in the microstructure.

## REFERENCES

[1] C. Park, S. Kim, Y. Kwon, Y. Lee, J. Lee, Mater. Sci. Eng. A **391**, 86 - 94 (2005).
[2] J.M. Bastidas, A. Forn, C.I. Torres, M.T. Polo, Mater. Corros. **52**, 691 - 696 (2001).
[3] S. Tahamtan, A. Fadavi Boostani, Mater. Des. **30**, 2483 - 2489 (2009).
[4] S. Tahamtan, A. Fadavi Boostani, Trans. Nonferrous Met. Soc. China **20**, 1702 – 1706 (2010).
[5] R. Władysiak, Arch Metall Mater. **52**, 229 (2007).
[6] R. Władysiak, Arch Metall Mater. **58**, 977 – 980, (2013).
[7] S. Fintová, R. Konečná, G.Nicoletto, Acta Met Slo **3**, 223 - 231 (2013).
[8] Sang Won Han, Met Mater. Int.**19**, 1 – 4 (2013)
[9] C. M. Dinnis, J. A. Taylor, and A. K. Dahle, Scripta Mater. **53**, 955 (2005).
[10] Yongzhong Zhang, Kui Zhang, Guojun Liu, Jun Xu, Likai Shi, Daijin Cui, Xuping Wu, Bo Cui, J Mater Process Tech. **137**, 195–200 (2003).
[11] Y.H. Cho, H.-C. Lee, K.H. Oh, A.K. Dahle, Metall Mater Trans A. **39**, 2435–2448 (2008).
[12] S. Haro-Rodríguez, R. E Goytia-Reyes, D. K. Dwivedi, V. H Baltazar-Hernández, H. Flores-Zúñiga, M. J. Pérez-López. Mater Design. **32**, 1865 – 1871 (2011).
[13] N.C.W. Kuijpers, W.H. Kool, P.T.G. Koenis, K.E. Nilsen, I. Todd, S. van der Zwaag, Materials Characterization **49,** 409-420 (2003).
[14] M. Warmuzek, J. Sieniawski, K. Wicher, G. Mrówka-Nowotnik, J Mater Process Tech **175**, 421 – 426 (2006).
[15] B. Bryksi Stunova, Acta Polytech. **52**, 26-32 (2012).
[16] R. Arrabal, B. Mingo, A. Pardo, M. Modedano, E. Matykina, I. Rodriguez, Corros Sci. **73,** 342 – 355 (2013).
[17] Kiryl A. Yasaku, M.L. Zheldkevich, S.V. Lamaka, M.G.S. Ferreira, Electrochim Acta **52,** 7651-7659 (2007).
[18] S.G. Shabestari, Mater. Sci. Eng. A **383**, 289-298 (2004).

*Received: 20 December 2014.*